DØ note 4371

Observation of semileptonic B decays to narrow D^{**} mesons

The DØ Collaboration
(Dated: March 19, 2004)

Using 250 pb^{-1} of integrated luminosity accumulated with the DØ detector during the period between April 2002 and January 2004, we observe semileptonic decays of $B \to \mu\nu D_1^0(2420)X$ and $B \to \mu\nu D_2^{*0}(2460)X$ and make a preliminary determination of the product branching rate :

$$Br(B \to \mu\nu(D_1^0(2420), D_2^{*0}(2460))X) \cdot Br(D_1^0(2420), D_2^{*0}(2460) \to \mathrm{D}^{*+}\pi^-) \;=\; (0.280 \pm 0.021(stat) \pm 0.088(syst))\%$$

where interference between the states is included.

Preliminary Results for Winter 2004 Conferences

I. INTRODUCTION

Orbitally excited states of the D meson are usually referred to as D** mesons. In the simplest case, D** mesons consist of a light quark and a charm quark in a state with orbital angular momentum $L = 1$. In the limit $m_c >> \Lambda_{QCD}$, the spin of the charm quark decouples from the other angular momenta and the angular momenta sum $j = S + L$ of the light quark spin S and the orbital angular momentum L is conserved. Thus, for $L = 1$ one expects one doublet of states with $j = 3/2$ and another doublet with $j = 1/2$.

We will use the following notations for D** mesons : D_0^{*0}, $D_1^{'0}$, $D_1^0(2420)$ and $D_2^{*0}(2460)$ where the first two states correspond to $j = 1/2$ and the last two to $j = 3/2$. Conservation of parity and angular momentum restricts the final states that are allowed in the decays of these four D** mesons. The states that decay through a D-wave are expected to be narrow ($20 \div 30$ MeV/c^2) while the states that decay through an S-wave are expected to be wide (several hundred MeV/c^2). $D_1^0(2420)$ and $D_2^{*0}(2460)$ decay through a D-wave and are, therefore, expected to be narrow. For a recent theoretical overview of the topic see Ref.[1]. The properties of the $L = 1$ states is summarized in Table I.

TABLE I: Properties of D** mesons with $L = 1$ [2]

State	J^P	$j = S + L$	Mass (MeV/c^2)	Width (MeV/c^2)	Decay Products
D_0^{*0}	0^+	1/2	-	-	$D\pi$
$D_1^0(2420)$	1^+	3/2	2422.2 ± 1.8	$18.9^{+4.6}_{-3.5}$	$D^*\pi$
$D_1^{'0}$	1^+	1/2	-	-	$D^*\pi$
$D_2^{*0}(2460)$	2^+	3/2	2458.9 ± 2.0	23 ± 5	$D\pi, D^*\pi$

The narrow D**mesons have been previously observed in several experiments, most recently at Belle [3] and BaBar [4].

The data set used for this analysis included approximately 250 pb^{-1} of integrated luminosity accumulated by the DØ detector between April 2002 and January 2004.

The DØ detector is comprised of the following main elements. A magnetic central-tracking system, which consists of a silicon microstrip tracker (SMT) and a central fiber tracker (CFT), both located within a 2 T superconducting solenoidal magnet [5]. The SMT has $\approx 800,000$ individual strips, with typical pitch of $50 - 150$ μm, and a design optimized for tracking and vertexing capability out to $|\eta| < 3$. The system has a six-barrel longitudinal structure, each with a set of four layers arranged axially around the beam pipe, and interspersed with 16 radial disks. The CFT has eight thin coaxial barrels, each supporting two doublets of overlapping scintillating fibers of 0.835 mm diameter, one doublet being parallel to the collision axis, and the other alternating by $\pm 3^\circ$ relative to the axis. Light signals are transferred via clear light fibers to solid-state photon counters (VLPC) that have ≈ 80 % quantum efficiency.

A muon system resides beyond the calorimetry, and consists of a layer of tracking detectors and scintillation trigger counters in front of 1.8 T toroids, followed by two more similar layers after the toroids. Tracking at $|\eta| < 1$ relies on 10 cm wide drift tubes [6], while 1 cm mini-drift tubes are used at $1 < |\eta| < 2$.

The trigger and data acquisition systems are designed to accommodate the large luminosity of Run II. Based on preliminary information from tracking, calorimetry, and muon systems, the output of the first level of the trigger is used to limit the rate for accepted events to ≈ 1.5 kHz. At the next trigger stage, with more refined information, the rate is reduced further to ≈ 800 Hz. These first two levels of triggering rely purely on hardware and firmware. The third and final level of the trigger, with access to all the event information, uses software algorithms and a computing farm, and reduces the output rate to ≈ 50 Hz, which is written to tape.

Information only from the muon and tracking systems was used in this analysis. The events were reconstructed using the p14 release of DØ software without particular trigger selections; however the majority of the selected events satisfied single muon trigger requirements. Typically the low p_T single muon triggers are prescaled at the first level of the trigger. The integrated luminosity quoted above does not take it into account and corresponds to the luminosity of the full DØ dataset.

Evidence of D** mesons was found in decays of $B \to \mu\nu \mathrm{D}^{*+}X$ as resonances in the $\mathrm{D}^{*+}\pi^-$ [10] invariant mass spectrum. D mesons were required to decay subsequently to $\mathrm{D}^{*+} \to \mathrm{D}^0\pi^+$ and $\mathrm{D}^0 \to K^-\pi^+$.

II. EVENT SELECTION

Muons were identified using standard DØ criteria Ref.[7]. For this analysis, muons were required to have hits in more than one muon chamber (nseg > 1), to have an associated track in the central tracking system with hits in

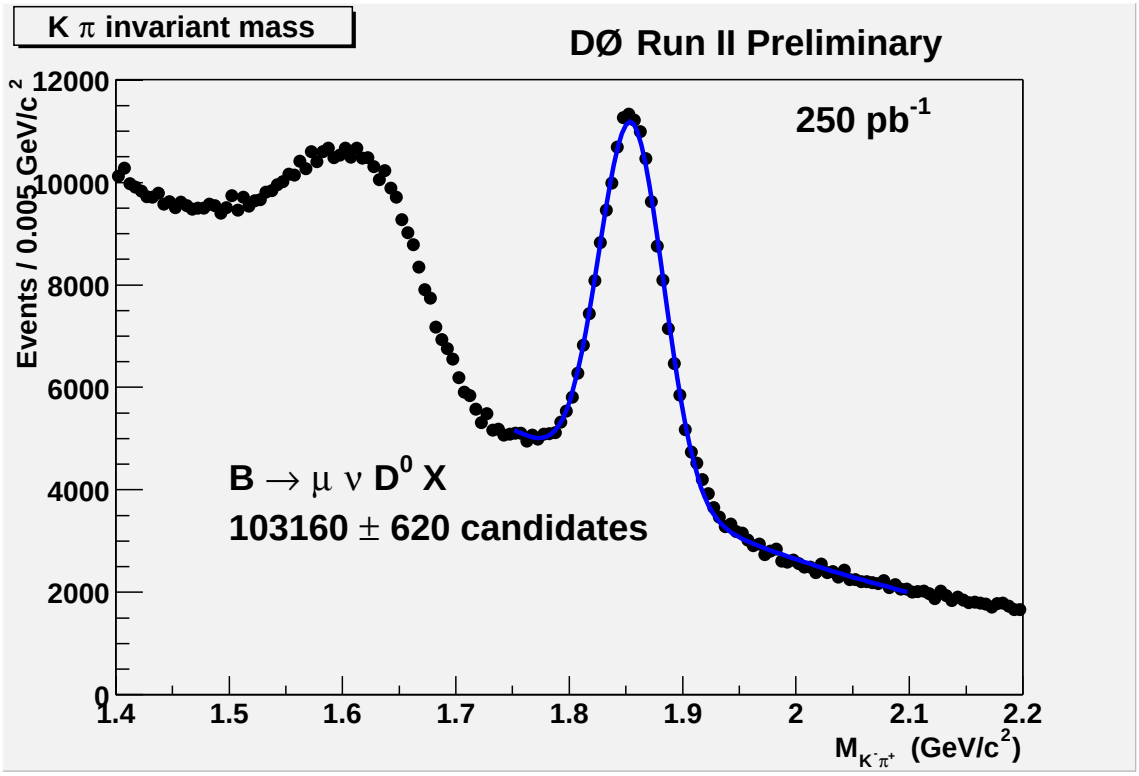

FIG. 1: The invariant mass of the $K\pi$ system for $\mu^- K^- \pi^+$ candidates. The curve shows the result of the fit of the $K^-\pi^+$ mass distribution with a Gaussian signal peak and polynomial background. The total number of D^0candidates in the peak is 103160 $\pm$ 620. The peak at lower masses corresponds to the partially reconstructed decay $D^0 \to K^-\pi^+X$ where typically a π^0 is not detected.

both SMT and CFT present, and to have transverse momentum $p_T^\mu > 2$ GeV/c, pseudo-rapidity $|\eta^\mu| < 2$, and total momentum $p^\mu > 3$ GeV/c.

All charged particles in the event were clustered into jets using the DURHAM clustering algorithm [8]. Events with more than one identified muon in the same jet were rejected, as well as the events with an identified $J/\psi \to \mu^+\mu^-$ decay.

A. Selections for D^0

The D^0 candidate was constructed from two particles of opposite charge included in the same jet as the reconstructed muon. Both particles should have hits in SMT and CFT, transverse momentum $p_T > 0.7$ GeV/c, and pseudo-rapidity $|\eta| < 2$. They were required to form a common D-vertex with fit $\chi^2_D < 9$. For each particle, the axial [11] ϵ_T and stereo [12] ϵ_L projections of track impact parameter with respect to the primary vertex together with the corresponding errors ($\sigma(\epsilon_T)$, $\sigma(\epsilon_L)$) were computed. The combined significance $\sqrt{(\epsilon_T/\sigma(\epsilon_T))^2 + (\epsilon_L/\sigma(\epsilon_L))^2}$ was required to be greater than 2. The distance d_T^D between the primary and D vertex in the axial plane was required to exceed 4 standard deviations: $d_T^D/\sigma(d_T^D) > 4$. The angle α_T^D between the D^0 momentum and the direction from the primary to the D^0 vertex in the axial plane was required to satisfy the condition: $\cos(\alpha_T^D) > 0.9$.

The tracks of muon and D^0 candidate were required to form a common B-vertex with fit $\chi^2_B < 9$. The momentum of the B candidate was computed as the sum of momenta of the μ and D^0. The mass of the $(\mu^- D^0)$ system was required to fall within $2.3 < M(\mu^- D^0) < 5.2$ GeV/c^2. If the distance d_T^B between the primary and B vertices in the axial plane exceeded $4 \cdot \sigma(d_T^B)$, the angle α_T^B between the B momentum and the direction from primary to B vertex in the axial plane was demanded to satisfy the condition $\cos(\alpha_T^B) > 0.95$. The distance d_T^B was allowed to be greater than d_T^D, provided that the distance between B and D vertices d_T^{BD} was less than $3 \cdot \sigma(d_T^{BD})$.

The mass spectrum of the $(K\pi)$ system after all these selections is shown in Fig.1. The masses of kaon and pion were assigned to particles according to the charge of the muon, requiring a $\mu^- K^- \pi^+$ final system.

The curve in Fig.1 shows the result of the fit of the $K^-\pi^+$ mass distribution with a Gaussian signal peak and

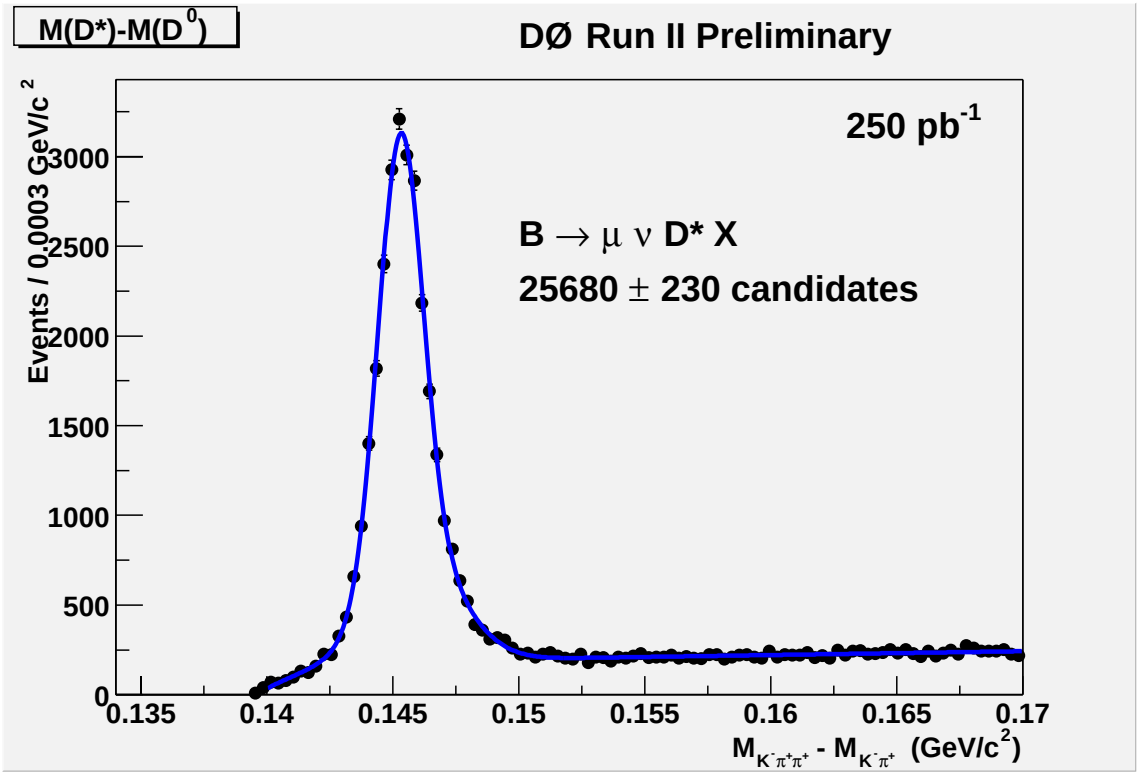

FIG. 2: The mass difference $M(\mathrm{D}^0\pi) - M(\mathrm{D}^0)$ for events with $1.75 < M(\mathrm{D}^0) < 1.95$ GeV/c^2. Total number of D* candidates is found to be 25680 ± 230. In the fit function the signal and the background have been approximated by sum of two Gaussian functions and by the sum of exponential and first order polynomial functions, respectively.

polynomial background. The total number of D^{0}candidates in the peak is 103160 ± 620. The peak at lower masses corresponds to the partially reconstructed decay $\mathrm{D}^0 \to K^-\pi^+X$ where typically a π^0 is not detected.

B. Selections for D*

For $\mu^-\mathrm{D}^0$ candidates, an additional pion with charge opposite to the charge of muon and with $p_T > 0.18$ GeV/c was searched for. Mass difference $\Delta M = M(\mathrm{D}^0\pi) - M(\mathrm{D}^0)$ for all such pions when $1.75 < M(\mathrm{D}^0) < 1.95$ GeV/c^2 is shown in Fig.2. The peak, corresponding to the production of $\mu^-\mathrm{D}^{*+}$ is clearly seen. The total number of D* candidates in the peak is equal to 25680 ± 230. The signal and the background have been modelled by a sum of two Gaussian functions and by the sum of exponential and first-order polynomial functions, respectively.

C. Selections for D**

D** candidates were selected by combining D* candidates with an additional pion, π^{**}. The D* candidates were selected in the D*- D^0 mass difference window between 0.142 and 0.149 GeV/c^2. The pion candidate had to have charge opposite to the charge of the D* candidate and have $p_T > 0.3$ GeV/c.

The pion from the D** decay can be selected by its topology since the corresponding track originates from the D* vertex rather then from the primary vertex. The impact parameters (IP) in the axial plane with respect to the primary and with respect to the D* vertex were determined for each track. The IP significance was defined as ratio of the impact parameter and its error. The ratio of IP significances for the primary and secondary vertex was required to be greater than 4 to select tracks belonging to the secondary vertex rather than to the primary vertex.

The B candidate was reconstructed from μ, D* and π^{**} particles. For all tracks used for the reconstruction of the B candidate, the number of SMT hits had to be greater than 1 and the number of CFT hits greater than 5. The decay length of the B meson was restricted to be smaller than 1 cm, the error on the B vertex had to be better than 0.5 mm, and χ^2 of the vertex fit had to be less than 25. The significance of the decay length of B meson in the axial

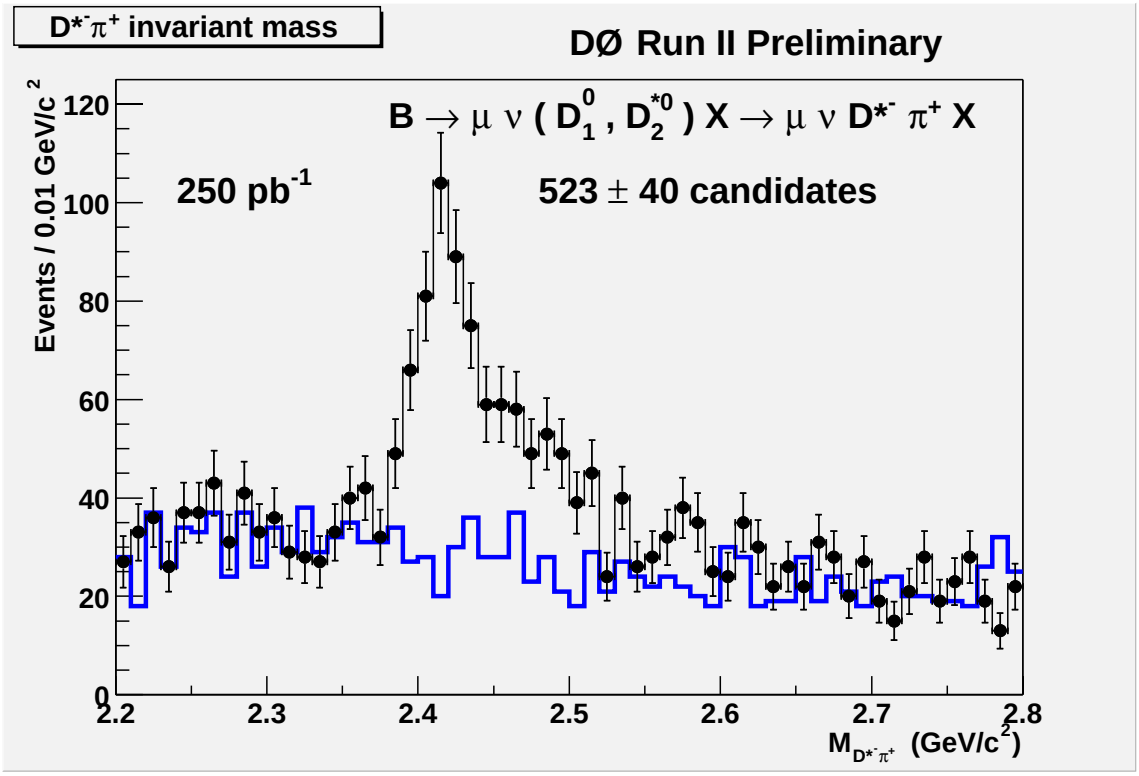

FIG. 3: The invariant mass $M(\mathrm{D}^{*-}\pi^{+})$ for events with selections described in the text. The points correspond to the $\mathrm{D}^{*}\pi$ combinations with opposite charges and the histogram corresponds to the same charge combinations. The total number of events in the peak is 523 ± 40, where the number of events was determined as the difference in the number of events for the right and wrong sign combinations in the range of $\mathrm{D}^{*}\pi$ invariant mass between 2.35 and 2.55 GeV/c^2.

plane was required to be greater than 3.

The D** invariant mass after all cuts is shown in Fig. 3. The points correspond to the $\mathrm{D}^{*}\pi$ combinations with opposite charges and the histogram corresponds to the same charge combinations. The mass peak in the region between 2.4 and 2.5 GeV/c^2 can be interpreted as two merged narrow D** states, $D_1^0(2420)$ and $D_2^{*0}(2460)$. The total number of events in the peak is 523 ± 40. The signal will be a combination of interfering Breit-Wigner functions, and for now the number of D** candidates was determined as difference in the number of events for the right and wrong sign combinations in the range of $\mathrm{D}^{*}\pi$ invariant mass between 2.35 and 2.55 GeV/c^2 in assumption that the background can be described by the wrong sign combination without any renormalization. In the future the separate amplitude for each state and relative phase will be extracted assuming they are two interfering Breit-Wigner resonances.

III. RESULTS

The branching rate for decays to D** can be determined by normalizing to the known values of branching rates to D* : $Br(B \to \mu\nu \mathrm{D}^{*+} X) = (2.75 \pm 0.19)\%$ and $Br(\mathrm{D}^{*+} \to \mathrm{D}^0\pi^+) = (67.7 \pm 0.5)\%$ [2].

$$Br(B \to \mu\nu(D_1^0(2420), D_2^{*0}(2460))X) \cdot Br(D_1^0(2420), D_2^{*0}(2460) \to \mathrm{D}^{*+}\pi^-) = Br(B \to \mu\nu \mathrm{D}^{*+} X) \cdot \frac{N_{D^{**}}^{data}}{N_{D^*}^{data}} \cdot \frac{1}{\epsilon^* \cdot Br(\mathrm{D}^{*+} \to \mathrm{D}^0\pi^+)} \cdot \frac{1}{\epsilon^*_{gen}}. \quad (1)$$

$N_{D^{**}}^{data}$ and $N_{D^*}^{data}$ are the numbers of D** and D* candidates as defined above. ϵ^* is the relative efficiency to reconstruct D** with respect to the reconstructed D* mesons and ϵ^*_{gen} is the efficiency correction factor accounting for different efficiency for D** and D* at the generator level due to the softer kinematic distributions of the D**.

TABLE II: Systematic errors

Source	Br absolute error	Br relative error
D^* branching rates	0.020%	7%
MC statistics	0.023%	8%
Normalization to D^*/D^0	0.023%	8%
$P_t^{\pi^{**}}$ dependence	0.052%	19%
Possible contribution from wide resonance	0.039%	14%
Possible interference effects of D_1^0 and D_2^{*0}	0.040%	14%
Different modelling of D^*fit	0.010%	4%
Trigger bias	0.020%	7%
Total systematic error	**0.088%**	**32%**

The efficiencies $\epsilon^* = (34.7 \pm 2.9)\%$, and $\epsilon^*_{gen} = (85 \pm 2)\%$, were determined from MC simulations using the standard DØ procedure : EvtGen generator interfaced to PYTHIA, followed by full GEANT modelling of the detector response, and then standard event reconstruction [9].

Using the inputs defined above :

$$Br(B \to \mu\nu(D_1^0(2420), D_2^{*0}(2460))X) \cdot Br(D_1^0(2420), D_2^{*0}(2460) \to D^{*+}\pi^-) = (0.280 \pm 0.021(stat))\%$$

The statistical error corresponds to the error on the total number of D^{**} in the mass peak. As defined the measured branching rate includes the quantum mechanical interference to identical $D^{*+}\pi^-$ states.

IV. SYSTEMATIC ERRORS

The systematic errors for the D^{**} branching rate are summarized in Table II.

All contributions to the systematic uncertainty can be divided into three main groups: uncertainties in the branching rates used for normalization, uncertainty in the MC modelling of efficiency, and uncertainties due to assumptions about the signal or background shape.

The contribution from $Br(B \to D^*\mu\nu X)$ and $Br(D^{*+} \to D^0\pi^+)$ to the systematic error was determined from the corresponding errors on these branching rates.

Two methods have been used to estimate the uncertainty in the MC efficiency. In the first method, the D^{**} branching rate has been calculated using two methods of normalization, first to D^* and then to D^0. The normalization to the D^0 branching rate was performed similarly to the D^* normalization described above. Difference in the results for the different methods of normalization may arise partly from the wrong estimate of efficiency in MC. Conservatively, the full difference was taken as a systematic error from this source.

To further estimate possible systematic effects from the non-ideal modelling of the signal efficiency in MC, the D^{**} sample was split into two halves : one with $P_T^{\pi^{**}} > 1$ GeV/c and one with $P_T^{\pi^{**}} < 1$ GeV/c. The branching rate has been determined independently for those two samples. The two results deviated from the result obtained with the full sample by $\pm$ 0.052%. Most of the deviation can be explained by the difference in the pion P_T spectrum between data and MC. This deviation was conservatively considered as the contribution to the systematic error from the uncertainty in the MC signal efficiency.

There are predictions and possibly observations [3] of a wide resonance with a mass of 2430 MeV/c^2 and a width of 380 MeV/c^2 predominantly decaying to $D^*\pi$. This resonance is not apparent in our data and it was not used in the estimation for the number of candidate events. However we evaluated a possible contribution from this resonance by fitting the narrow D^{**} signal with two Gaussians and allowing a third Gaussian in the fit function with the central value and sigma fixed to the wide resonance parameters. To decrease the variation of background that can mimic the effect of the wide resonance, we approximated the background with a straight line with slope determined from the fit of the combinatorial background of opposite sign. The normalization of the background was allowed to float in one case and was fixed to the value determined from the fit of the background in the other case. Comparing the number of events in the two narrow resonances with and without the presence of the third wide resonance, the systematic uncertainty due to this assumption was estimated to be equal to 0.039%.

Another possible systematic effect related to the shape of the two resonances can originate from the interference between $D_1^0(2420)$ and $D_2^{*0}(2460)$. The constructive or destructive interference can result in different behavior of

the tails of the invariant mass distribution. This uncertainty has been estimated comparing the efficiency of the D^{**} invariant mass window selection used to determine the total number of events in the mass peak for different assumptions about the phase of the interference. The two resonances were modelled by two Breit-Wigner functional forms with an abitrary phase between them convoluted with a Gaussian of the detector mass resolution. The uncertainty of 0.040% was determined as difference between two estreme cases corresponding to fully constructive or fully destructive interference between the resonances.

The systematic error due to the D^* fitting procedure was estimated by fitting the D^* mass peak and the corresponding background with different functions.

The candidate events were recorded by a variety of single muon triggers. The single muon triggers normally have a p_T threshold and a difference in the muon p_T spectrum of D^{**} and D^* can result in different trigger efficiency to the corresponding signals. The resulting trigger bias was estimated comparing muon p_T spectra in the MC simulations of D^* and D^{**} and performing the calculation of the D^{**} branching rate for the muon p_T cut raised to 4 GeV/c.

All the above sources were assumed to be not correlated and the total systematic error of 0.088% was found by summing the errors in quadrature.

V. DISCUSSION

According to available LEP results [2], we have the branching rate

$$Br(B \to \mu\nu \mathrm{D}^{*+}\pi^- X) = (0.48 \pm 0.10)\%.$$

These measurements were based on topological searches and did not distinguish between resonant and non-resonant contributions. Our result, therefore, for the first time determines the component of the $B \to \mu\nu \mathrm{D}^{*+}\pi^- X$ process proceeding through the narrow D^{**} states. We have determined that this component constitutes slightly more than one half of the total rate.

VI. CONCLUSIONS

Using 250 pb^{-1} of integrated luminosity accumulated with the DØ detector during the period between April 2002 and January 2004, we have observed semileptonic decays of $B \to \mu\nu D_1^0(2420)X$ and $B \to \mu\nu D_2^{*0}(2460)X$ and made a preliminary determination of the product branching rates of

$$Br(B \to \mu\nu(D_1^0(2420), D_2^{*0}(2460))X) \cdot Br(D_1^0(2420), D_2^{*0}(2460) \to \mathrm{D}^{*+}\pi^-) \;=\; (0.280 \pm 0.021(stat) \pm 0.088(syst))\%,$$

where interference between the states is included.

Acknowledgments

We thank the staffs at Fermilab and collaborating institutions, and acknowledge support from the Department of Energy and National Science Foundation (USA), Commissariat à L'Energie Atomique and CNRS/Institut National de Physique Nucléaire et de Physique des Particules (France), Ministry for Science and Technology and Ministry for Atomic Energy (Russia), CAPES, CNPq and FAPERJ (Brazil), Departments of Atomic Energy and Science and Education (India), Colciencias (Colombia), CONACyT (Mexico), Ministry of Education and KOSEF (Korea), CONICET and UBACyT (Argentina), The Foundation for Fundamental Research on Matter (The Netherlands), PPARC (United Kingdom), Ministry of Education (Czech Republic), Natural Sciences and Engineering Research Council and WestGrid Project (Canada), BMBF (Germany), A.P. Sloan Foundation, Civilian Research and Development Foundation, Research Corporation, Texas Advanced Research Program, and the Alexander von Humboldt Foundation.

[1] Z.Ligetti "Introduction to heavy meson decays and CP asymmetries" hep-ph/0302031.
[2] Particle Data Group, K. Hagiwara *et al.*, Phys. Rev. **D66**, (2002) 010001.
[3] Belle collaboration "Study of $B^- \to D^{**0}\pi^-$ decays" hep-ex/0307021.

[4] Babar collaboration "Study of decays $B^- \to D^{*+}\pi^-\pi^-$"hep-ex/0308026.
[5] V. Abazov, et al., in preparation for submission to Nucl. Instrum. Methods Phys. Res. A, and T. LeCompte and H.T. Diehl, "The CDF and DØ Upgrades for Run II", Ann. Rev. Nucl. Part. Sci. **50**, 71 (2000).
[6] S. Abachi, *et al.*, Nucl. Instrum. Methods Phys. Res. A **338**, 185 (1994).
[7] muon ID web page
[8] S.Catani, Yu.L.Dokshitzer, M.Olsson, G.Turnock, B.R.Webber, Phys.Lett. **B269** (1991) 432.
[9] T.Sjöstrand et. al. hep-ph/0108264
EvtGen / D0mess webpage http://www-clued0.fnal.gov/d0_mess/
[10] Charge conjugate states are implied throughout the note
[11] plane perpendicular to the beam direction
[12] parallel to the beam direction